DOI 10.5012/bkcs.2011.32.8.2705

Enhanced Carbon Dioxide Adsorption on Post-Synthetically Modified Metal-Organic Frameworks

Nakeun Ko and Jaheon Kim*

*Department of Chemistry, Soongsil University, Seoul 156-743, Korea. *E-mail: jaheon@ssu.ac.kr*
Received June 7, 2011, Accepted June 30, 2011

Four MOFs functionalized with **1**-Me, **1**-Pr, **1**-Ph, and **1**-PhCF$_3$ were prepared through post-synthetic modifications of a metal-organic framework (MOF), UMCM-1-NH$_2$ (**1**) with acetic, butyric, benzoic, and 4-(trifluoromethyl)benzoic anhydrides, respectively. Methane adsorption measurements between 253 and 298 K at pressures up to 1 bar indicated that both **1**-Ph and **1**-PhCF$_3$ adsorbed more CH$_4$ than the parent MOF, **1**. All the functionalized MOFs adsorbed more CO$_2$ than **1** under conditions similar to the CH$_4$ test. The introduction of functional groups promoted adsorption of both CH$_4$ and CO$_2$ despite significantly reducing Brunauer-Emmet-Teller (BET) surface area: 4170 (**1**), 3550 (**1**-Me), 2900 (**1**-Pr), 3680 (**1**-Ph), and 3520 m^2/g (**1**-PhCF$_3$). Electron-withdrawing aromatic groups (**1**-Ph, **1**-PhCF$_3$) more effectively enhanced CO$_2$ adsorption than electron-donating alkyl groups (**1**-Me, **1**-Pr). In particular, **1**-Ph adsorbed 23% more CO$_2$ at 298 K and 50% more at 253 K than **1**.

Key Words : Metal-organic framework, Post-synthetic modification, Adsorption, Methane, Carbon dioxide

Introduction

Metal-organic frameworks (MOFs) – structures of metal ions connected to organic linkers through coordination bonds – can achieve very large Brunauer-Emmet-Teller (BET) surface areas of over 4000 m^2/g.[1-6] Large surface areas generally aid MOFs to act as gas adsorbents and catalysis. To enhance the effectiveness of very porous MOFs for recognizing target adsorbents or substrates, their framework surfaces can be optimized or functionalized.[7] For this, post-synthetic modification of MOFs can easily introduce various functional groups, allowing tuning of pore properties.[8,9] Various post-synthetic modifications have been recently reported.[10] For example, post-synthetic modification of microporous IRMOF-3 and DMOF-1 could control or improve the pore properties of the parent MOFs.[11-15] Both MOFs have 2-aminoterephthalate (BDC-NH$_2$) linkers, the amino groups of which can react with extrinsic modifiers such as organic anhydrides. A similar approach has also been applied to mesoporous UMCM-1-NH$_2$ using benzoic anhydride, producing UMCM-1-AMPh with increased hydrogen storage capacity at 77 K and 1 bar compared with the original UMCM-1-NH$_2$.[15]

UMCM-1-NH$_2$ (**1**), formulated as Zn$_4$O(BTB)$_{4/3}$(BDC-NH$_2$), has a similar structure to UMCM-1 (Zn$_4$O(BTB)$_{4/3}$(BDC)), though the BDC in UMCM-1 is replaced by BDC-NH$_2$ in **1**.[3,15] These MOFs show unique N$_2$ isotherms at 77 K, exhibiting a clear step starting at $P/P_0 = 0.2$, attributable to the filling of the pores of the hexagonal channels that have 2.4 nm × 2.9 nm openings. Therefore, gas adsorption at pressures lower than $P/P_0 = 0.2$ is largely due to the fused microporous cages (1.4 nm × 1.7 nm) that form the wall of the large channel (Fig. 1). As the BDC-NH$_2$ linkers are located at the junctions of the microporous cages (Fig. 1), the introduction of small functional groups to the linkers through post-synthetic modification would mainly affect the pore environment of the cages, without affecting the porosity of the large channel.

The capture and short-term storage of CO$_2$ are potentially important processes for mitigating climate change or purifying

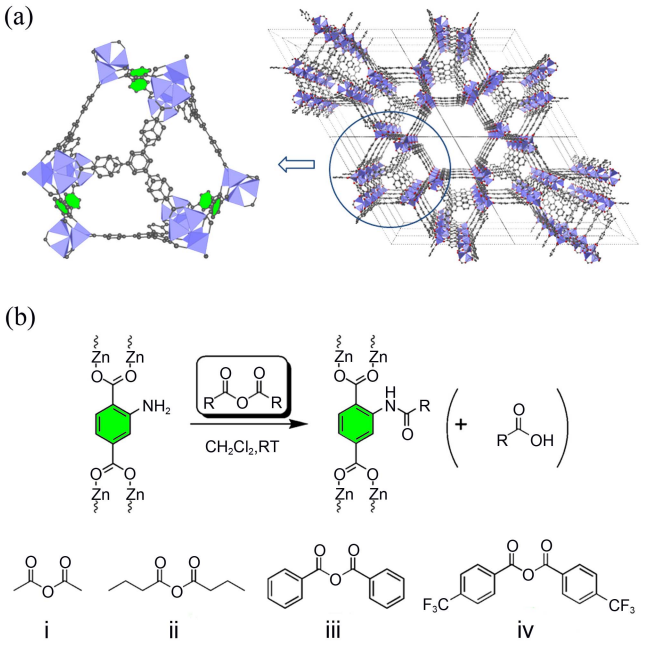

Figure 1. (a) Structure of UMCM-1-NH$_2$ (**1**) and its cage; Zn$_4$O units are shown as blue tetrahedra, and six BDC-NH$_2$ linkers are shown as green hexagons. The disordered -NH$_2$ groups are not shown; crystal coordinates are from ref. 13. (b) The post-synthetic modification of **1** with anhydrides to prepare functionalized MOFs, **1**-R, and the anhydrides used: i) acetic anhydride for **1**-Me, ii) butyric anhydride for **1**-Pr, iii) benzoic anhydride for **1**-Ph, and iv) 4-(trifluoromethyl)benzoic anhydride for **1**-PhCF$_3$.

natural gas. Therefore, many approaches have been investigated to increase CO_2 adsorption by MOFs, for example open-metal sites, framework interpenetration, flexible frameworks, interactions with amines, and polar framework surfaces.[16] This work reports the tuning of CO_2 adsorption properties through functionalizing pores using functional groups with different inductive effects: electron-donating alkyl groups and electron-withdrawing aryl groups. Four MOFs (**1**-R, where R is Me, Pr, Ph, or $PhCF_3$) were prepared through the post-synthesis modification of **1** with acetic, butyric, benzoic, and 4-trifluoromethyl phenyl anhydrides, respectively (Fig. 1). Pr is a better electron-donating group than Me, and $PhCF_3$ is a better electron-withdrawing group than Ph. CO_2 adsorption isotherms of the MOFs were measured at 253, 273, and 298 K and at pressures up to 1 bar. Methane adsorption measurements were also conducted for comparison as both gases have similar polarizabilities but very different quadrupole moments.[16] **1**-Ph and **1**-$PhCF_3$, functionalized by electron-withdrawing aromatic groups, were more effective CO_2 adsorbents than **1**-Me and **1**-Pr, modified by electron-donating alkyl groups.

Experimental

Chemicals. Acetic anhydride, butyric anhydride, 2-amino-terephthalic acid (H_2BDC-NH_2), dichloromethane, *N*,*N*-dimethylformamide (DMF), and zinc nitrate hexahydrate ($Zn(NO_3)_2{\cdot}6H_2O$) were purchased from Sigma-Aldrich. Benzoic anhydride and 4-(trifluoromethyl)benzoic anhydride were purchased from TCI. All starting materials were used without further purifications. H_3BTB (4,4′,4″-benzene-1,3,5-triyl-tribenzoic acid) was prepared according to a published procedure.

Physical Measurements. Elemental analyses were carried out on an EA 1110, CE instrument. IR spectra were recorded on a JASCO FT/IR-4000 spectrophotometer with samples prepared as KBr pellets. ^{1}H-NMR spectra of digested MOF crystals in DCl/DMSO were obtained on a Bruker 400 MHz NMR spectrometer. X-ray powder diffraction (XRPD) data were collected on a Rigaku MiniFlex diffractometer with Cu Kα radiation (λ = 1.5418 Å).

Gas Adsorption Measurements. Adsorption isotherms of N_2, CO_2 and CH_4 at pressures up to 1 bar were measured by standard volumetric procedures on BELSORP-mini (BEL-Japan, INC.) equipment. Each sample was dried and fully outgassed at 160 ºC under vacuum (< 1.0×10^{-3} torr) for 6 hr immediately before measurement. The dead volume of the sample cell was automatically measured using helium gas. Pressure equilibrium points were also collected automatically by the equipment. Each sample's weight was measured without exposing it to air. Using nitrogen isotherm points below $P/P_0 = 0.20$, BET surface areas were determined by the equation provided by the manufacturer. During CH_4 and CO_2 adsorption measurements, sample cells were maintained at 253 K in a dry ice/acetone bath, at 273 K in an ice/water bath, or at 298 K in a water bath. Plots of isosteric heats of adsorption were calculated using a virial equation; zero-coverage values were regarded as each MOF's heat of adsorption.

Syntheses.

UMCM-1-NH_2 (1): H_3BTB (0.127 g, 0.29 mmol), H_2NH_2BDC (0.147 g, 0.811 mmol), and $Zn(NO_3)_2{\cdot}6H_2O$ (0.850 g, 2.86 mmol) were dissolved in DMF (30 mL). The reaction mixture was heated at 95 ºC in a capped vial for 48 hr to give brown needle-shaped crystals (**1**). These were filtered and washed with neat DMF (5 × 30 mL) and dichloromethane (5 × 30 mL). The crystals were stored in dichloromethane for further use. Anal. Calcd (%) for the evacuated sample, $Zn_4O(C_{27}H_{15}O_6)_{4/3}(C_8H_5NO_4)$: C, 48.99; H, 2.77; N, 1.30. Found: C, 49.00; H, 2.91; N, 1.31. FT-IR (KBr pellet, 4000-400 cm^{-1}): 3353 (br, w), 1585 (vs), 1541 (vs), 1406 (vs), 1253 (w), 1184 (w), 1109 (w), 1016 (m), 854 (m), 811 (w), 780 (s), 705 (m), 672 (w), 584 (w), 484 (w). ^{1}H-NMR spectrum (400 MHz, DCl/DMSO-d_6, δ): 8.10 (s, 4H), 8.07 (s, 16H), 7.79 (d, J = 8.4 Hz, 1H), 7.45 (s, 1H), 7.11 (d, J = 8.4 Hz, 1H).

1-Me: Before its post-synthesis modification, **1** was washed again with dichloromethane and evacuated under reduced pressure (< 1.0×10^{-3} Torr) for 6 hr at 160 ºC. Each batch reaction used *ca.* 30 mg sample in 1.0 mL stock solution prepared by dissolving acetic anhydride (f.w. 102.09, 2.0 mL) in 100 mL dichloromethane. After one day, the crystals were filtered and washed with neat dichloromethane (3 × 5 mL) to remove the produced acetic acid. They were then placed in 1.0 mL fresh stock solution for one more day. This procedure was conducted a third time to complete the modification of **1** with acetic anhydride. Finally, the crystals were washed with neat dichloromethane (3 × 5 mL) and left in neat dichloromethane for 48 hr to remove un-reacted species. Anal. Calcd (%) for the evacuated sample, $Zn_4O(C_{27}H_{15}O_6)_{4/3}(C_{10}H_7NO_5)$: C, 49.33; H, 3.08; N, 1.25. Found: C, 49.31; H, 3.16; N, 1.41. FT-IR (KBr pellet, 4000-400 cm^{-1}): 3266 (br, w), 1585 (vs), 1544 (vs), 1407 (vs), 1304 (w), 1250 (w), 1184 (w), 1016 (m), 855 (m), 811 (w), 779 (s), 704 (m), 672 (w), 484 (w). ^{1}H-NMR (400 MHz, DCl/DMSO-d_6, δ): 9.03 (s, 1H), 8.10 (s, 4H), 8.07 (s, 16H), 7.68(d, J = 8.4 Hz, 1H), 2.16 (s, 3H).

1-Pr: The post-synthetic modification was similar to that for **1**-Me. A stock solution was prepared by dissolving butyric anhydride (f.w. 158.19, 2.0 mL) in 100 mL dichloromethane. Three modification steps were conducted and the complete conversion of **1** to **1**-Pr took six days. Anal. Calcd (%) for the evacuated sample, $Zn_4O(C_{27}H_{15}O_6)_{4/3}(C_{12}H_{11}NO_5)$: C, 50.46; H, 3.08; N, 1.23. Found: C, 50.47; H, 3.05; N, 1.22. FT-IR (KBr pellet, 4000-400 cm^{-1}): 3265 (br, w), 1585 (vs), 1543 (vs), 1408 (vs), 1184 (w), 1108 (w), 1016 (m), 960 (w), 854 (m), 811 (w), 779 (s), 705 (m), 672 (w), 562 (w), 507 (w). ^{1}H-NMR (400 MHz, DCl/DMSO-d_6, δ): 9.03 (s, 1H), 8.10 (s, 4H), 8.07(s, 16H), 7.67 (d, J = 8.4 Hz, 1H), 2.38 (t, J = 7.2 Hz, 2H), 1.65 (q, J = 7.2 Hz, 2H), 0.94 (t, J = 7.2 Hz, 3H).

1-Ph: The post-synthetic modification was similar to that for **1**-Me. Instead of making a stock solution, anhydride solution was prepared for each reaction step by dissolving benzoic anhydride (f.w. 226.23, 47.5 mg) in 1.0 mL dichloro-

methane. The complete conversion of **1** to **1**-Ph required three post-synthetic modification steps and took nine days. Anal. Calcd (%) for the evacuated sample, $Zn_4O(C_{27}H_{15}O_6)_{4/3}$ ($C_{15}H_9NO_5$): C, 50.63; H, 3.05; N, 1.16. Found: C, 50.63; H, 3.10; N, 1.13. FT-IR (KBr pellet, 4000-400 cm^{-1}): 3247 (br, w), 1584 (vs), 1542 (vs), 1407(vs), 1305 (w), 1252 (w), 1184 (w), 1016 (m), 963 (w), 854 (m), 811 (w), 779 (s), 705 (m), 562 (w), 486 (w). ^{1}H-NMR (400 MHz, DCl/DMSO-d_6, δ): 9.27 (s, 1H), 8.13 (d, J = 6.8 Hz, 1H), 8.10 (s, 4H), 8.07 (s, 16H), 7.97(d, J = 7.2 Hz, 2H), 7.75 (d, J = 6.8 Hz, 1H), 7.67 (t, J = 4.8 Hz, 1H), 7.62 (t, J = 7.2 Hz, 2H).

1-PhCF$_3$: The post-synthetic modification was similar to for **1**-Ph. Anhydride solution was prepared for each reaction step by dissolving 4-(trifluoromethyl)benzoic anhydride (f.w. 362.22, 76.1 mg) in 1.0 mL dichloromethane. The complete conversion of **1** to **1**-Ph required three post-synthetic modification steps and took six days. Anal. Calcd (%) for $Zn_4O(C_{27}H_{15}O_6)_{4/3}(C_{16}H_8NO_5F_3)$: C, 50.42; H, 2.54; N, 1.13. Found: C, 50.41; H, 2.50; N, 1.11. FT-IR (KBr pellet, 4000-400 cm^{-1}): 3264 (br, w), 1584 (vs), 1543 (vs), 1409 (vs), 1326 (m). 1252 (w), 1171 (m), 1128 (m), 1065 (m), 1015 (m), 899 (w), 855 (m), 811 (w), 779 (s), 706 (m), 509 (w). ^{1}H-NMR (400 MHz, DCl/DMSO-d_6, δ): 9.18 (s, 1H), 8.15 (d, J = 8.0 Hz, 2H), 8.14 (d, J = 8.0 Hz, 1H), 8.09 (s, 4H), 8.06 (s, 16H), 7.99 (d, J = 8.0 Hz, 2H), 7.77 (d, J = 8.0 Hz, 1H).

Results and Discussion

Syntheses and Characterization. **1**-Me, **1**-Pr, and **1**-Ph have been previously reported as UMCM-1-AM1, UMCM-1-AM3, and UMCM-1-AMPh, respectively by Cohen *et al.*.[14,15] In this work, these materials were prepared by modified procedures and dichloromethane solvent. **1**-Ph was produced with a higher conversion yield. During the reactions, crystals in the reaction batch were collected and analyzed by ^{1}H-NMR to monitor the degree of conversion. Conversions were generally 85-90% after the first reaction step, ~95% after the second, and > 99% after the third. All the functionalized MOFs could be quantitatively obtained, though with markedly different reaction times: **1**-Me, 3 days; **1**-Pr, 6 days; **1**-Ph, 9 days; **1**-PhCF$_3$, 6 days. While it took 3 days to obtain both **1**-Me and UMCM-1-AM1, the reaction time for **1**-Pr was much longer than that for UMCM-1-AM3. The preparation of **1**-Ph had reaction conditions very different from those for UMCM-1-AMPh, which had a conversion yield of ~76%. **1**-Ph was obtained quantitatively over 9 days at room temperature in dichloromethane, whereas UMCM-1-AMPh was prepared by heating the reaction mixture for one day at 55 °C in chloroform.

PXRD patterns of all the samples were consistent throughout the course of the reaction, indicating that their periodic structures were not affected during the reactions (Fig. 2). The ^{1}H-NMR spectra showed evidence of successful modifications. The signals attributed to the H_2BDC-NH-R linkers shifted significantly down-field compared with those of H_2BDC-NH_2 (Fig. 3). Elemental analysis showed good agreement with the formulae of all the modified MOFs, within allowable errors, supporting the quantitative modification of the parent MOF, **1**.

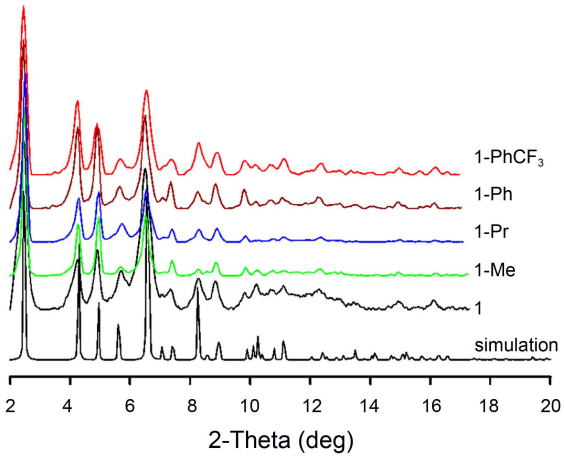

Figure 2. PXRD patterns of the functionalized and original MOFs.

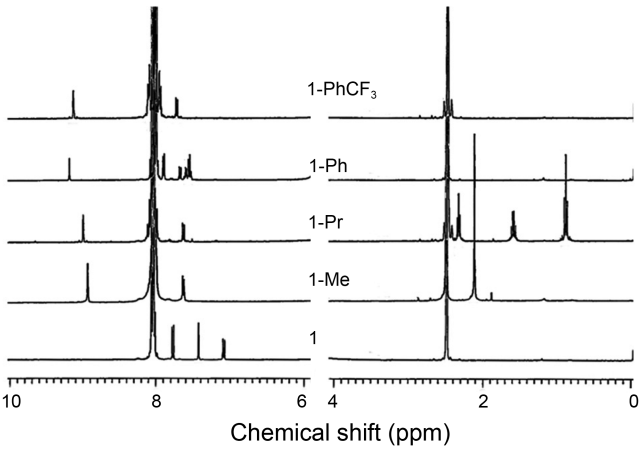

Figure 3. ^{1}H-NMR spectra of the original and functionalized MOFs measured in DCl/DMSO-d_6. The large signals commonly observed at 8.1 ppm are attributable to H_3BTB. Broad water signals were observed between 4 and 6 ppm; for clarity, they are not shown.

N_2 Adsorption Measurements. The nitrogen sorption isotherm of the four functionalized MOFs showed clear second steps at P/P_0 = 0.2, similar to **1** (Fig. 4). However, each functionalized MOF showed different heights of the first step, suggesting that the modifications had produced micropores different from **1**. The amounts of N_2 adsorbed by each MOF were similar in the second step. This suggests that the introduction of functional groups to **1** did not perturb the mesoporous channels, only the microporous cages. An independent structural study suggested that the large channel of **1** could be altered only by the modification with alkyl chains longer than dodecane. Therefore, it is not strange that the N_2 adsorption isotherms of the functionalized MOFs showed large decreases in N_2 uptake only at lower pressures.

The BET surface areas of the MOFs in this work were predicted to correlate with the mass of the frameworks: **1** > **1**-Me > **1**-Pr > **1**-Ph > **1**-PhCF$_3$. However, the surface areas

Table 1. Formula weights and measured surface areas of the MOFs in this work. Parentheses show changes (%) in f.w. and BET surface areas relative to **1**

MOF		Surface area (m^2/g)	
Name	f.w. (g/mol)	BET	Langmuir
1	1037	4170	6020
1-Me	1079 (+4.1)	3550 (−14.9)	5100
1-Pr	1107 (+6.8)	2900 (−30.5)	4180
1-Ph	1141 (+10.0)	3680 (−11.8)	5300
1-$PhCF_3$	1209 (+16.6)	3520 (−15.6)	5100

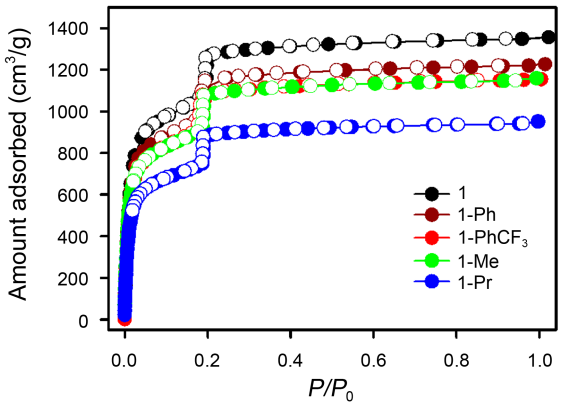

Figure 4. N_2 adsorption isotherms of the original and functionalized MOFs at 77 K. The filled and open circles respectively correspond to adsorption and desorption.

of the modified samples were reduced by *ca.* 12-31% compared with that of **1**, in decreasing order: **1** > **1**-Ph > **1**-Me ~ **1**-$PhCF_3$ > **1**-Pr, i.e.: 4170 (**1**), 3550 (**1**-Me), 2900 (**1**-Pr), 3680 m^2/g (**1**-Ph), and 3520 m^2/g (**1**-$PhCF_3$) (Table 1). Increases of framework weight did not directly correlate with the reduction of surface area; therefore, changes of framework volume or pore size are not considered here to avoid possible ambiguities. The aromatic groups of **1**-Ph and **1**-$PhCF_3$ appear to have provided more adsorptive sites for nitrogen molecules than the alkyl groups of **1**-Me and **1**-Pr. Similar was observed for UMCM-1-AMPh, which could adsorb more hydrogen than UMCM-1-NH_2.

CH_4 Adsorption Measurements. CH_4 and CO_2 adsorption isotherms of **1** and the four modified MOFs were measured at 253, 273, and 298 K at pressures up to 1 bar. These measurements were expected to reveal the temperature-dependence of the MOFs' gas adsorption behaviors, and show which functional groups would be preferable for CO_2 adsorption. The CH_4 adsorption results can aid the understanding of how the introduced functional groups affect the MOFs. Because CH_4 has similar polarizability to CO_2 but lacks a quadrupole moment, it shows different adsorption behavior from CO_2 that has a large quadrupole moment. The results can be used to elucidate the roles of the introduced functional groups in improving CO_2 adsorption.

At every tested temperature, the uptake of CH_4 at $P/P_0 = 1$ by the functionalized MOFs was correlated with their BET surface area. CH_4 uptake amounts: **1**-Ph > **1**-$PhCF_3$ > **1**-Me >

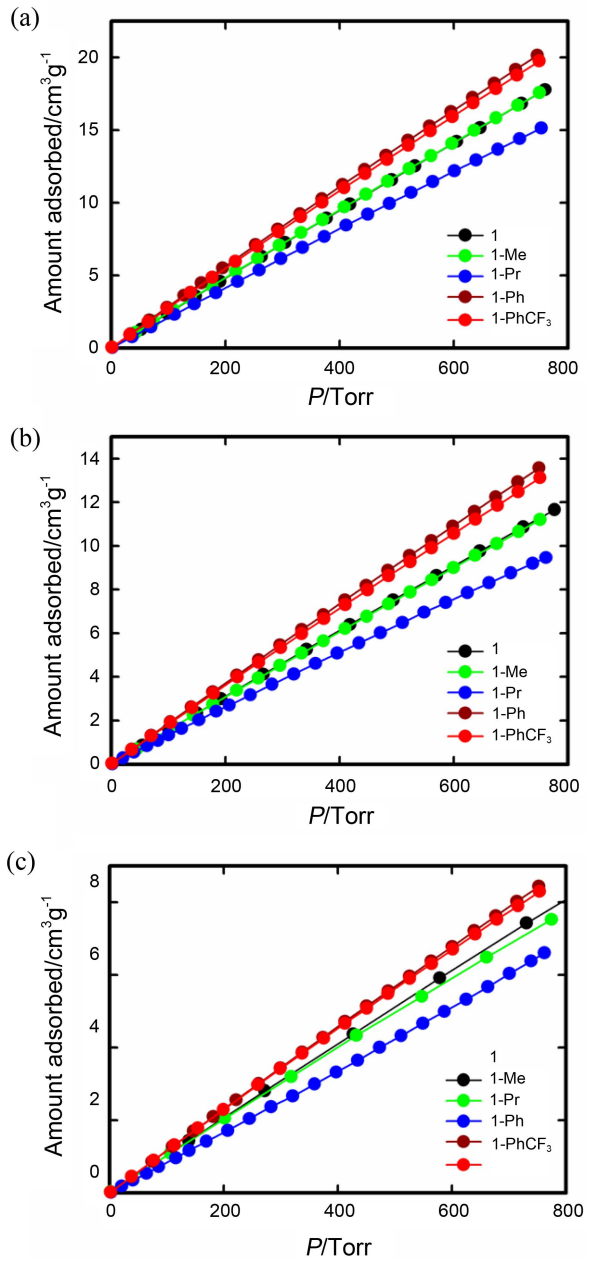

Figure 5. CH_4 sorption isotherms for **1**, **1**-Me, **1**-Pr, **1**-Ph, and **1**-$PhCF_3$ measured at (a) 253 K, (b) 273 K, and (c) 298 K. For clarity, only the adsorption branch points are shown; all the isotherms were reversible.

Table 2. CH_4 uptakes of the original and functionalized MOFs at different temperatures. Parentheses indicate changes (%) relative **1**. The isosteric enthalpies of adsorption extrapolated to zero coverage were calculated using virial-type equations

MOF	CH_4 uptake amounts (mg/g)			ΔH_{ads} (kJ/mol)
	253 K	273 K	298 K	
1	12.7	8.3	5.5	11.4
1-Me	12.6 (−1.2)	8.0 (−3.8)	5.4 (−2.1)	12.2
1-Pr	10.8 (−14.9)	6.8 (−18.8)	4.7 (−14.1)	11.5
1-Ph	14.4 (+13.3)	9.7 (+16.5)	6.0 (+9.7)	12.7
1-$PhCF_3$	14.1 (+11.1)	9.4 (+12.6)	5.9 (+7.9)	12.3

1-Pr *vs*. BET surface areas, **1**-Ph > **1**-Me ~ **1**-$PhCF_3$ > **1**-Pr (Fig. 5, Table 2). This is in accordance with what was expected from the nitrogen adsorption experiments. That is, that the aromatic groups of **1**-Ph and **1**-$PhCF_3$ aided CH_4 adsorption more than the alkyl groups of **1**-Me and **1**-Pr. **1**-$PhCF_3$, with a surface area similar to that of **1**-Me, adsorbed significantly more CH_4 than **1**-Me. This simple correlation does not apply when **1** is considered in the series with the functionalized MOFs. Adsorbed amounts of CH_4: **1**-Ph > **1**-$PhCF_3$ > **1** > **1**-Me > **1**-Pr. This does not match the surface area trend because **1** had the largest surface area of the MOFs in this work.

The modification of **1** with aromatic functional groups was more effective at lower temperature. **1**-Ph could adsorb 13.4% more CH_4 than **1** at 253 K, and only 9.1% more at 298 K. As temperature increased, bulkier groups appeared to experience more thermal motion than smaller groups. This reduced the strength of interaction with CH_4, although the effect was small. The relative changes in CH_4 uptake as temperature increased from 253 K to 298 K were −56.7% (**1**), −57.1% (**1**-Me), −56.5% (**1**-Pr), −58.3% (**1**-Ph), and −58.2% (**1**-$PhCF_3$). UMCM-1 was reported to have an isosteric enthalpy of adsorption of 6.5 kJ/mol. Therefore, the increased adsorption enthalpy of UMCM-1-NH_2 (**1**), 11.4 kJ/mol, is attributable to the presence of NH_2 groups in the framework. Similarly, the increased enthalpies of the functionalized MOFs (11.5-12.7 kJ/mol) were due to the introduction of the functional groups. These increases were achieved despite the decreased surface areas of the functionalized MOFs.

CO_2 Adsorption Measurements. Similar to CH_4 adsorption, aromatic groups better aided CO_2 adsorption than alkyl groups. However, all the functionalized MOFs showed greater CO_2 uptakes than **1** at every tested temperature: **1**-Ph > **1**-$PhCF_3$ > **1**-Me > **1**-Pr > **1** (Fig. 6, Table 3). The CO_2 adsorption capacity of the functionalized MOFs increased significantly compared with the increases of CH_4 adsorption. For example, **1**-Ph adsorbed 50% more CO_2 than **1** at 253 K, and 23% more at 298 K, whereas its increases in CH_4 adsorption relative to **1** at the same temperatures were only 13.4% and 9.1%, respectively. The trend in the change of the CO_2 adsorption capacity with temperature was similar to that of CH_4 adsorption. The relative changes of CO_2 uptake by the MOFs as temperature increased from 253 K to 298 K were −66.0% (**1**), −68.9% (**1**-Me), −70.5% (**1**-Pr), −72.3% (**1**-Ph), and −71.1% (**1**-$PhCF_3$).

Although the average change of the MOFs' CO_2 adsorption (−69.8%) was much greater than that (−57.4%) for CH_4 in this work, the average isosteric enthalpy for CO_2 (17.9 kJ/mol) is significantly larger than that of CH_4 (12.0 kJ/mol). This is presumed to be due the quadrupole moment of CO_2, which introduces an adsorption interaction that is dependent on the relative orientation of the adsorptive sites and CO_2. This interaction may be diminished as the temperature increased due to increased thermal motion of the organic linkers.

CO_2 adsorption enthalpies are usually greater than those of CH_4 for most sorbents such as zeolites, activated carbons,

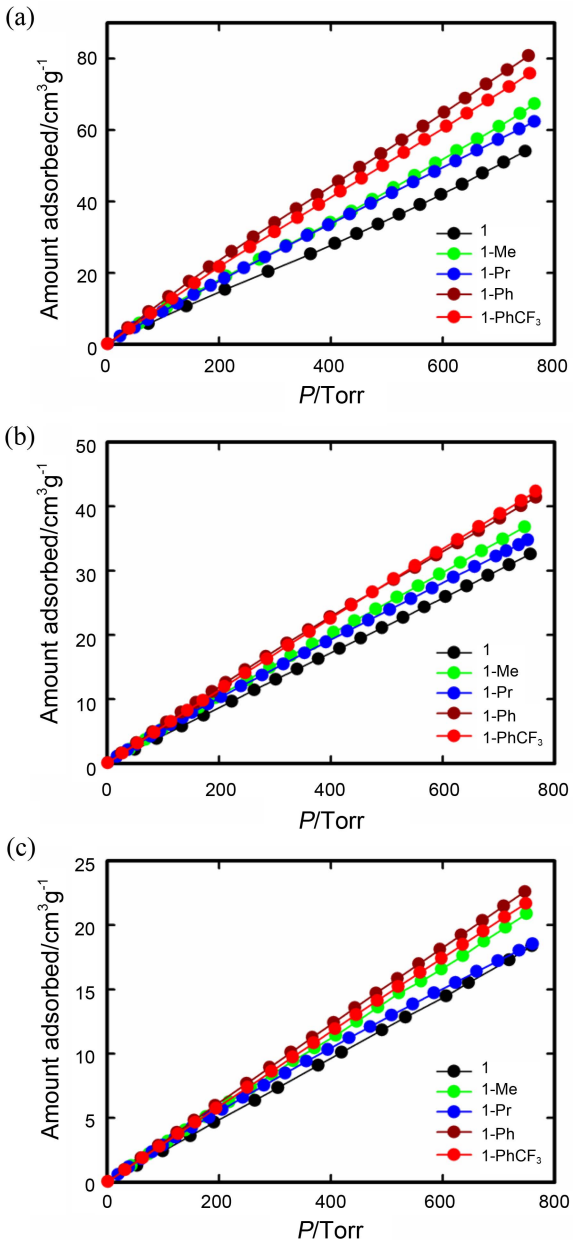

Figure 6. CO_2 adsorption isotherms for **1**, **1**-Me, **1**-Pr, **1**-Ph, and **1**-$PhCF_3$ measured at (a) 253 K, (b) 273 K, and (c) 298 K. For clarity, only adsorption branch points are shown; all the isotherms were reversible.

Table 3. CO_2 uptake of the original and functionalized MOFs at different temperatures. Parentheses indicate changes (%) relative to **1**. Isosteric enthalpies of adsorption extrapolated to zero coverage were calculated using virial-type equations

MOF	CO_2 uptake amounts (mg/g)			ΔH_{ads} (kJ/mol)
	253 K	273 K	298 K	
1	106	64	36	16.3
1-Me	132 (+29)	72 (+13)	41 (+14)	17.3
1-Pr	122 (+15)	68 (+7)	36 (+0)	17.7
1-Ph	159 (+50)	81 (+27)	44 (+23)	19.6
1-$PhCF_3$	149 (+40)	83 (+30)	43 (+18)	18.8

and MOFs.[18] These results follow this trend. The isosteric heat of CO_2 adsorption for **1**-Ph was 19.6 kJ/mol, much smaller than those of MOFs with open metal sites, for example, MIL-100 (63 kJ/mol), COP-27-Ni (*ca.* 42 kJ/mol),[19] and Mg-MOF-74 (39 kJ/mol),[20] but was larger than that of UMCM-1 (11.9 kJ/mol).[18] When compared with UMCM-1, the increased CO_2 adsorption enthalpies of the MOFs in this work can be largely attributed to the presence of amino or amide groups, as demonstrated by aminoMIL-53(Al) (38.4 kJ/mol) and MIL-53(Al) (20.1 kJ/mol).[21] The differences between the MOFs must be due to the introduced functional groups.

As mentioned above, MOFs' structural factors can increase interactions with CO_2, for example open-metal sites, framework interpenetration, flexible frameworks, amines in the frameworks, and polar framework surfaces.[16] Among these, the last two are related to the MOFs in this work. This is because of the amine (-NH_2) groups in **1** and the amide groups (-NHCOR) in the functionalized MOFs that have different functional groups, which exert varying local polarity. However, common amide functionality alone cannot explain the differences in the MOFs' adsorption enthalpies of CH_4 (12.0 kJ/mol) and CO_2 (17.9 kJ/mol). All the functionalized MOFs were better adsorbents for CO_2 than **1**, whereas only **1**-Ph and **1**-$PhCF_3$ were better adsorbents of CH_4. Therefore, considering that CO_2 is more sensitive than CH_4 towards polar surfaces, it was shown that the modification of **1** with anhydrides increased the local polarity of the MOF framework surfaces. Aromatic groups were better modifiers than alkyl groups to improve the CO_2 affinity of **1** because in addition to producing favorable adsorptive sites, aromatic, electron-withdrawing, groups can provide more polar framework surfaces than alkyl, electron-donating, groups.

Conclusions

Four MOFs (**1**-Me, **1**-Pr, **1**-Ph, and **1**-$PhCF_3$) were prepared by post-synthesis reactions of a very porous MOF, UMCM-1-NH_2 (**1**), and corresponding anhydrides. The MOFs' BET surface areas were not correlated with the mass increases in their frameworks. Predicted BET surface areas: **1** > **1**-Me > **1**-Pr > **1**-Ph > **1**-$PhCF_3$; observed BET surface areas: **1** > **1**-Ph > **1**-Me ~ **1**-$PhCF_3$ > **1**-Pr. This indicates that the aromatic groups provided more adsorptive sites for nitrogen molecules.

CH_4 and CO_2 adsorption measurements were conducted at 253, 273, and 298 K at pressures up to 1 bar to investigate the effects of the modifications. At every tested temperature, adsorbed amounts of CH_4 were ranked: **1**-Ph > **1**-$PhCF_3$ > **1** > **1**-Me > **1**-Pr. In contrast, CO_2 uptake was ranked: **1**-Ph > **1**-$PhCF_3$ > **1**-Me > **1**-Pr > **1**. These observations show that post-synthetic modification could enhance affinity for both CH_4 and CO_2. Also, both alkyl and aromatic groups increased local polarity, enhancing CO_2 adsorption. The aromatic electron-withdrawing groups enhanced CO_2 uptake more than the electron-donating alkyl groups.

Acknowledgments. This research was performed for the CDRS, one of the 21st Century Frontier R&D Programs funded by the Ministry of Education, Science and Technology of Korea.

References

1. Wong-Foy, A. G.; Matzger, A. J.; Yaghi, O. M. *J. Am. Chem. Soc.* **2006**, *128*, 3494-3495.
2. Llewellyn, P. L.; Bourrelly, S.; Serre, C.; Vimont, A.; Daturi, M.; Hamon, L.; Weireld, G. D.; Chang, J.-S.; Hong, D.-Y.; Hwang, Y. K.; Jhung, S. H.; Férey, G. *Langmuir* **2008**, *24*, 7245-7250.
3. Koh, K.; Wong-Foy, A. G.; Matzger, A. J. *Angew. Chem. Int. Ed.* **2008**, *47*, 677-680.
4. Koh, K.; Wong-Foy, A. G.; Matzger, A. J. *J. Am. Chem. Soc.* **2009**, *131*, 4184-4185.
5. Furukawa, H.; Ko, N.; Go, Y. B.; Aratani, N.; Choi, S. B.; Choi, E.; Yazaydin, A. O.; Snurr, R. Q.; O'Keeffe, M.; Kim, J.; Yaghi, O. M. *Science* **2010**, *239*, 424-428.
6. Farha, O. K.; Yazaydın, O.; Eryazici, I.; Malliakas, C.; Hauser, B.; Kanatzidis, M. G.; Nguyen, S. T.; Snurr, R. Q.; Hupp, J. T. *Nature Chem.* **2010**, *2*, 944-948.
7. Holst, J. R.; Cooper, A. I. *Adv. Mater.* **2010**, *22*, 5212-5216.
8. Wang, Z.; Cohen, S. M. *Chem. Soc. Rev.* **2009**, *38*, 1315-1329.
9. Kasinathan, P.; Seo, Y.-K.; Shim, K.-E.; Hwang, Y. K.; Lee, U-H.; Hwang, D.-W.; Hong, D.-Y.; Halligudi, S. B.; Chang, J.-S. *Bull. Korean Chem. Soc.* **2011**, *32*, 2073-2075.
10. Tanabe, K. K.; Cohen, S. M. *Chem. Soc. Rev.* **2011**, *40*, 498-519.
11. Wang, Z.; Cohen, S. M. *J. Am. Chem. Soc.* **2007**, *129*, 12368-12369.
12. Wang, Z.; Cohen, S. M. *J. Am. Chem. Soc.* **2009**, *131*, 16675-16677.
13. Tanabe, K. K.; Wang, Z.; Cohen, S. M. *J. Am. Chem. Soc.* **2008**, *130*, 8508-8517.
14. Wang, Z.; Tanabe, K. K.; Cohen, S. M. *Inorg. Chem.* **2009**, *48*, 296-306.
15. Wang, Z.; Tanabe, K. K.; Cohen, S. M. *Chem. Eur. J.* **2010**, *16*, 212-217.
16. D'Alessandro, D. M.; Smit, B.; Long, J. R. *Angew. Chem. Int. Ed.* **2010**, *49*, 6058-6082.
17. Choi, S. B.; Seo, M. J.; Cho, M.; Kim, Y.; Jin, M. K.; Jung, D.-Y.; Choi, J.-S.; Ahn, W.-S.; Rowsell, J. L. C.; Kim, J. *Cryst. Growth Des.* **2007**, *7*, 2290-2293.
18. Mu, B.; Schoenecker, P. M.; Walton, K. S. *J. Phys. Chem. C* **2010**, *114*, 6464-6471.
19. Dietzel, P. D. C.; Johnsen, R. E.; Fjellvåg, H.; Bordiga, S.; Groppo, E.; Chavanc, S.; Blom, R. *Chem. Commun.* **2008**, 5125-5127.
20. Britt, D.; Furukawa, H.; Wang, B.; Glover, T. G.; Yaghi, O. M. *Proc. Natl. Acad. Sci. USA* **2009**, *106*, 20637-20640.
21. Couck, S.; Denayer, J. F. M.; Baron, G. V.; Rémy, T.; Gascon, J.; Kapteijn, F. *J. Am. Chem. Soc.* **2009**, *131*, 6326-6327.